

# Numerical Modelling of a Three-Story Building Using a Hybrid of Mass Timber Walls with Buckling-Restrained Braces

Gustavo A. Araújo R. (□), Barbara Simpson, Tu X. Ho, Gustavo F. Orozco O., Andre R. Barbosa, and Arijit Sinha

Oregon State University, Corvallis, OR 97331, USA gustavo. araujo@oregonstate.edu

Abstract. Mass timber buildings are gaining popularity in North America as a sustainable and aesthetic alternative to traditional construction systems. However, several knowledge gaps still exist in terms of their expected seismic performance and plausible hybridizations with other materials, e.g. steel energy dissipators. This research explores the potential use of mass plywood wall panels (MPP) in spine systems using steel buckling-restrained braces (BRBs) as energy dissipators. The proposed BRB-MPP spine assembly makes up the lateral load-resisting system of a three-story mass-timber building segment that will be tested under cyclic quasi-static loading at Oregon State University. The specimen geometry and material properties result in BRBs that are shorter and of smaller core area than in most common steel structural applications. Small BRBs are prone to exhibit a hardened compressive response and fracture due to ultra-low-cycle fatigue when subjected to repeated cycles of large strain amplitude. These issues, along with the limited availability of test data, make small BRBs difficult to model. To support the experimental testing program, a material model with combined kinematic and isotropic hardening is calibrated against the available experimental data for three BRB specimens to estimate the behavior of BRBs of short length (≤3,500 mm [138 in]) and small core area  $(<2,600 \text{ mm}^2 \text{ [4 in}^2\text{]})$ , similar to the ones designed for the test specimen. The calibrated model is used to predict the behavior of the BRB-MPP spine experiment.

**Keywords:** Buckling-restrained brace  $\cdot$  Mass timber  $\cdot$  Spine system  $\cdot$  Numerical model

#### 1 Introduction

Mass timber shear walls used in conjunction with energy dissipators are candidates to conform hybrid spine systems due to their high strength-to-weight ratio and stiffness. A spine system consists of a vertical elastic element that helps to distribute lateral deformations more evenly with building height. Recent research has explored the use of buckling-restrained braces (BRBs) as energy dissipating hold-downs in mass timber 1 walls [1], which can yield and maintain strength in both tension and compression. In these systems, the vertically-oriented BRBs are the only elements designed to undergo

inelastic deformations while the spine components (i.e. the shear wall and the connections to the BRBs) are designed to remain essentially elastic. However, due to strength requirements in connecting BRBs to mass timber and geometry considerations, the selected brace can often have shorter length and smaller core area relative to the ones used in steel buckling-restrained braced frames (BRBFs) (e.g. [1, 2]). The shorter yield length can result in larger strain demands on the BRBs and potentially larger force demands transferred to the spine due to increased strain hardening effects, usually characterized by means of adjustment factors ( $\beta$ ,  $\omega$ ).

To support the design of mass timber spines employing BRBs, numerical models need to be developed that are capable of simulating asymmetric kinematic and isotropic strain hardening observed in various BRB specimens. However, many existing models are calibrated to the cyclic behavior of BRBs with larger core areas and longer yield lengths than what are expected in hybrid mass timber-BRB systems, such as the widely used material *Steel4* model [3] available in OpenSees [4].

This research numerically explores mass plywood panels (MPP) used as pinsupported shear walls combined with BRBs to achieve enhanced performance goals, herein referred to as a BRB-MPP spine system. As a case study, a three-story building segment was designed with a BRB-MPP spine system as its lateral force-resisting system (LFRS). The design of the BRBs was supported by the re-calibration of the parameters used in the *Steel4* material model to the experimental data of three specimens, representative of the core area and yield length of BRB used in the three-story building segment. The calibrated numerical model was used to predict the cyclic behavior of the BRB-MPP spine system under quasi-static loading, which will be tested in 2022 at Oregon State University.

## 2 Building Archetype and Test Specimen

The building archetype is a three-story building, representative of office building construction in Seattle, WA. A two-bay by two-bay segment of this building was selected to be tested under cyclic quasi-static loading at Oregon State University (OSU). Testing will be carried out in the main direction of the building only. The LFRS includes a hybrid of 203-mm thick MPP walls and BRBs attached to the bottom corners as hold-downs, herein referred to as the hybrid BRB-MPP spine. The spine is located between the two mid gravity frames composed of LVL beams and columns; see Fig. 1(a). The spine was designed to remain elastic to impose a uniform distribution of lateral deformations in the building. The design also allows the wall to pivot and uplift at the base, while ensuring proper shear transfer to the foundation. This base condition mimics a compressive-only pin support, with the BRBs entirely resisting the base moment and the wall resisting the base shear; see Fig. 1(b).

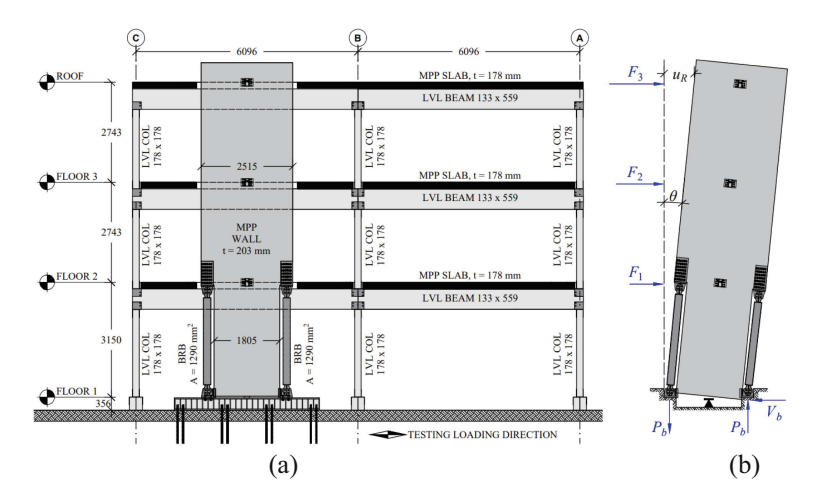


**Fig. 1.** (a) Elevation view of the mid gravity frame and the hybrid BRB-MPP spine. (b) Idealized distribution of forces in the spine.

### 3 BRB Design

The core area of the BRB energy dissipators was selected to meet the axial force demands,  $P_b$ , from code-prescribed seismic loads corresponding to the design base shear,  $V_{b,DE}$ , and a response modification coefficient, R=8, consistent with BRB-Frame systems [5]. On the other hand, the length of the BRBs was governed by displacement and stiffness considerations. Due to the pin support conditions of the MPP wall (see Fig. 1(b)), only the axial stiffness of the BRBs and the shear stiffness of the wall contribute to the first-story stiffness. To keep story drift ratios below 2.0% at the design level [5], the length of the BRBs was selected to correspond approximately to the first-story height. To ensure adequate ductility of the BRBs under ultra-low cycle fatigue, the BRBs were additionally sized based on maximum strain demands in the yielding region of the brace, herein assumed not to exceed 2.5% strains at a roof drift ratio of 2.0%.

#### 4 Numerical Model of BRBs

The force demands imposed by the BRBs in the end connections and the mass timber spine depend on the strain demands and the resulting kinematic and isotropic hardening of the BRBs. To support the design of the BRB-MPP spine specimen and prediction of the behavior for the experimental testing program, a phenomenological model was used to model the BRBs. The material model used for this model was calibrated to available experimental data of three BRB specimens with geometry features and strain demands resembling the BRB used in the hybrid BRB-MPP spine system.

### 4.1 Model Description

The BRBs were modeled with a truss element, with additional stiff elements at its ends representing the end connection regions [6]. The truss element has length and stiffness that represents the global response of the brace, including both the yielding and transition regions. Because the inelastic response of a BRB is restricted to the yielding region of the brace, a stiffness modification factor, Q, was used to account for the transition regions of larger area within the BRB core. The factor Q was computed according to Simpson [6], which assumes the transition and yielding regions are in series. The connection regions are not included in the computation of Q because these are explicitly accounted in the modelling scheme. The modification factor is then applied to the material stiffness,  $\hat{E} = QE$ .

To represent asymmetric kinematic and isotropic hardening of BRBs in tension and compression, the Menegotto-Pinto uniaxial model, extended by Zsarnóczay [3] as *Steel4* in OpenSees, was utilized for the truss element. This model accounts more realistically for the cumulative plastic deformation as the controlling variable for isotropic hardening compared to other extensions of the Menegotto-Pinto model. As the default parameters recommended by Zsarnóczay [3] were calibrated to a database of mainly medium to large BRBs of intermediate yield length, the BRB model was recalibrated to simulate smaller core areas and the potentially larger strain demands of BRBs used in the hybrid BRB-MPP spine system.

When subjected to repeated cycles of large amplitude plastic deformations, BRBs can exhibit ultra-low-cycle fatigue. In BRBs with short yield lengths, increased strain demands can make estimates of fatigue life even more critical. Low-cycle fatigue of the BRBs is estimated by accumulating damage using Miner's rule and estimation of fracture using a Coffin-Manson log-log relationship [7]. The strength and stiffness of the BRB becomes negligible after a damage level of 1.0 is reached.

#### 4.2 Test Data

The material model used for the truss was calibrated to the experimental data of three BRB specimens. The selected specimens were considered representative of the BRB used in the hybrid BRB-MPP, as they were from similar manufactures and featured short length ( $\leq 3,500$  mm [138 in]) and small core area ( $\leq 2,600$  mm<sup>2</sup> [4 in<sup>2</sup>]); see Table 1. In particular: [i] CB225 is most similar to the BRB used in the hybrid BRB-MPP spine specimen, [ii] PC160 had a small core area and a varied loading protocol of large followed by small displacement cycles, and [iii] NCBF-3SB is subjected to fewer cycles of larger strain amplitudes, exhibited BRB rupture, and has total and yielding lengths ( $r_T$  and  $r_y$ ) resembling the BRB used in the hybrid BRB-MPP spine specimen.

Specimen	BRB at OSU		
PC160 [8] NCBF-B-3SB [6]		CB225*	
285	276	290	276
2,452	3,226	1,452	1,290
4.0	7.7	2.5	_
6,401	3,505	4,445	2,972
4,470	1,930	3,111	2,032
0.70	0.55	0.70	0.68
Pinned	Welded	Pinned	Bolted
	PC160 [8] 285 2,452 4.0 6,401 4,470 0.70	PC160 [8] NCBF-B-3SB [6] 285 276 2,452 3,226 4.0 7.7 6,401 3,505 4,470 1,930 0.70 0.55	PC160 [8] NCBF-B-3SB [6] CB225* 285 276 290 2,452 3,226 1,452 4.0 7.7 2.5 6,401 3,505 4,445 4,470 1,930 3,111 0.70 0.55 0.70

Table 1. Specimens used for BRB modeling calibration and BRB-MPP spine specimen.

### 4.3 Optimized Calibration

A minimization study was conducted to automatically calibrate the BRB material model. The optimization procedure minimized the sum of the squared  $L^2$ -norm of the error in the simulated and experimentally measured axial force response of each BRB, normalized by the number of points from the load history used to compute the error,  $N_i$ :

$$\min \sum_{i=1}^{N_{lests}} \sum_{n=1}^{N_i} \frac{\left(\mathbf{f}_n^{\mathbf{s}} - \mathbf{f}_n^{\mathbf{e}}\right)^{\mathrm{T}} \left(\mathbf{f}_n^{\mathbf{s}} - \mathbf{f}_n^{\mathbf{e}}\right)}{N_i^2} \tag{1}$$

 $N_{tests}$  = number of specimens used in the calibration (in this case, three);  $N_i$  = number of characteristic points;  $\mathbf{f}_n^{\mathbf{e}}$  and  $\mathbf{f}_n^{\mathbf{s}}$  = experimentally measured and simulated brace strength at characteristic point, n, in the load history. To weigh the most important parts of the hysteretic shape, errors were computed only at select characteristic points in the loading protocol: (a) zero displacement, (b) three-quarters of the displacement amplitudes, (c) zero load, and (d) peak load amplitudes, resulting in ten critical points per cycle. No critical points were selected from cycles after BRB rupture occurred.

The minimization procedure was carried out in Python 3.9 using the *fmin* function from *scipy.optimize*. Because *Steel4* is highly customizable, overfitting becomes a potential issue due to the large number of parameters and limited availability of test data. To reduce the number of parameters, only the isotropic hardening parameters were calibrated (i.e.  $b_i$ ,  $b_l$ , and  $\rho_i$  in tension and compression; see model documentation [3]). The constraints used to bound the optimized parameters to realistic values and the resulting optimized parameters are shown in Table 2 and Table 3. The obtained values of  $b_i$  are generally smaller than the default values for the three BRBs studied.

Comparisons of the experimental and numerical results using the optimized parameters are plotted in Fig. 2. The simulated behavior agrees with the experimental data, with the best estimate for specimen CB225. In CB225 and PC160, the model overpredicts the tension side and slightly underpredicts the compression side. For transitions from large to small strain amplitude cycles, the tested PC160 exhibits a decrease in the size of the yielding surface. The current implementation of *Steel4* cannot account for this type of behavior. Finally, the calibrated model for specimen

<sup>\*</sup> Data from the same manufacturer as the BRB at OSU

Constraints	Parameter (in tension and					
	compression)					
	$b_i$	$b_l$	$ ho_{i,t}$	$ ho_{i,c}$		
Lower bound	0.001	0.0001	1.0	0.5		
Upper bound	0.01	No larger than $b_i$	2.5	1.5		

Table 2. Optimization constraints.

Table 3. Optimized BRB material model.

Direction	Kinematic hardening			Isotropic hardening				Fatigue				
	$b_k$	$R_0$	$r_1$	$r_2$	$b_i$	$b_l$	$\rho_i$	$R_i$	$l_{yp}$	$\epsilon_0^*$	m	$\varepsilon_{max}^{*}$
Tens	0.003	25	0.91	0.15	0.0028	0.0001	2.30	1.0	1.0	0.19	-0.46	0.05
Compr	0.023				0.0042	0.0001	0.87					

<sup>\*</sup> Fatigue strain parameters need to be adjusted by  $r_T/r_v$ .

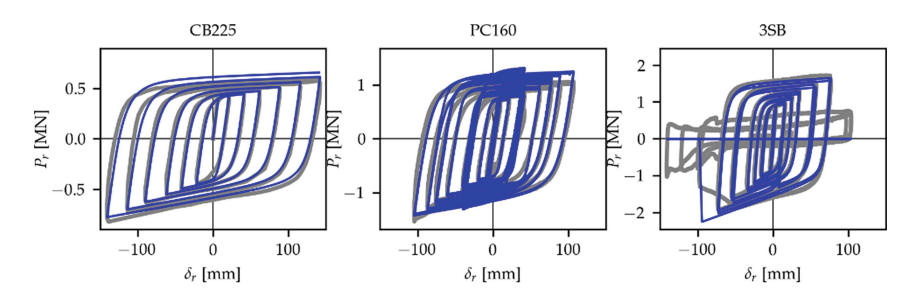


Fig. 2. BRB calibration to proprietary BRB experiments.

NCBF-B-3SB (termed 3SB in Fig. 2) slightly overestimates the compressive strength and underestimates the tension strength in large-amplitude cycles, but the global predicted response is in good agreement with the experimental data, including the prediction of failure.

# 5 Simulated Cyclic Behavior of the Test Specimen

The calibrated BRB model was used to develop a nonlinear model in OpenSees to predict the cyclic behavior of the hybrid BRB-MPP spine system when subjected to a modified version of the CUREE protocol. The numerical model only includes the hybrid MPP-BRB spine and neglects the gravity system and the diaphragms; see Fig. 3 (a).

Force-based beam-column elements with fiber sections were used to model the flexural behavior of the MPP, following a *Hinge-Radau* integration scheme. The constitutive behavior of the MPP fibers was idealized as elastic-perfectly plastic in

compression, and linear-elastic in tension. The shear response was also idealized as linear. The assigned material properties are consistent with previous experimental testing [9].

The base support conditions of the uplifting spine were simulated with zero-length elements that were near-rigid in shear and compression but had near-zero stiffness in tension. No rotational rigidity was assigned to the base condition, as it was assumed that only the BRBs resist the base moment demand while the MPP resists all the shear forces. The BRBs were modeled with corotational trusses and the previously calibrated material properties. To appropriately model the distance between the BRBs, the trusses were connected to the MPP spine using stiff horizontal elastic beam-column elements.

Figure 3(b) shows the predicted cyclic response of the spine up to a level of roof drift ratio  $(\theta_{roof})$  of 4%. The onset of yielding in the BRBs starts at  $\theta_{roof} = 0.5\%$  corresponding to a base shear of  $V_b = 121 \, \mathrm{kN} \, [27 \, \mathrm{kip}]$ . Continued strain hardening of the BRBs is predicted until the end of the analysis, with an ultimate strength of 177 kN [40 kip] at  $\theta_{roof} = 4.0\%$ . The distribution of story drift remains near-uniform after yielding, as expected in spine systems subjected to a first-mode force distribution.

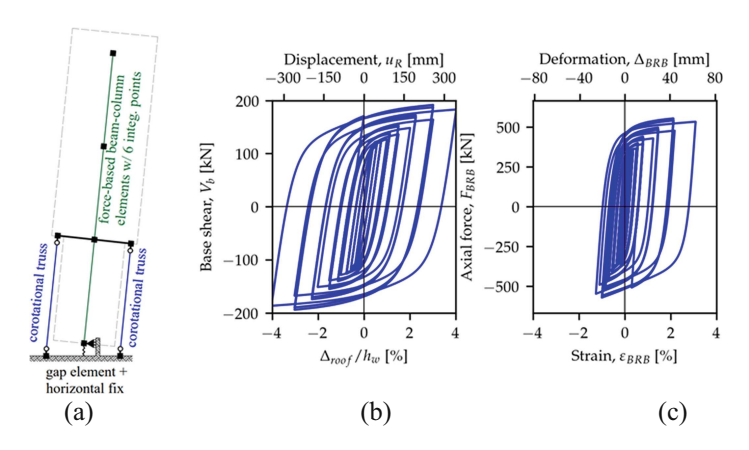


**Fig. 3.** Simulated behavior of the hybrid BRB-MPP spine: (a) modeling scheme, (b) global cyclic load – displacement history, and (b) local BRB force-deformation history.

Figure 3(c) shows the observed local response in the BRBs. Strain demands in the braces are about three times larger in tension than in compression. To ensure equilibrium, the brace in tension and compression must exhibit the same axial force. As BRBs are stronger in compression, the BRB in tension is subjected to larger deformations to develop the same force. The maximum force demand imposed by the BRB to the spine is 580 kN [130 kips], which agrees with the force demands estimated in the design stage. No fracture in the BRBs is predicted based on the low-cycle fatigue model.

Note that the actual behavior of the specimen may differ from this prediction due to different phenomena not accounted in this study, such as the flexibility in the

connections of the BRB to the MPP and the BRB to base, as well as the base shear key. Further studies will also include the interactions between the spine and the gravity system.

#### 6 Conclusions

A nonlinear model in OpenSees was calibrated to an experimental database of three BRB specimens, representative of braces of small core areas and short lengths used as hold-downs in mass timber applications. The model adequately simulated the asymmetric isotropic and kinematic strain hardening and rupture of the three specimens. Though the experimental database is limited in size, the model is deemed adequate for the nonlinear analysis of a hybrid BRB-MPP spine. The calibrated model was used to predict the cyclic behavior of the spine under quasi-static loading. However, some errors in the BRB model were noted that are worth further exploring; particularly, the predicted continued hardened strength upon unloading to smaller amplitude cycles.

**Acknowledgments.** The authors would like to thank CoreBrace, BoiseCascade, Simpson Strong-Tie, and Freres Lumber Co for advising in the design of the three-story building segment and donating materials. This project was executed under the USDA ARS Award No. 58-0204-9-165. The findings, opinions, recommendations, and conclusions in this paper are those of the authors alone and do not necessarily reflect the views of the sponsors.

#### References

- Massari M, Savoia M, Barbosa AR (2017) Experimental and numerical study of two-story post-tensioned seismic resisting CLT wall with external hysteretic energy dissipaters. In: Atti del XVII convegno anidis l'ingegneria sismica in Italia: Pistoia, 17–21 settembre 2017. Studi in tema di internet ecosystem Pisa University Press, Pisa
- Zimmerman RB et al (2020) Catalyst a mass timber core wall building with high ductility hold-downs in a Seismic Region. In: 2020 world conference on timber engineering. Santiago, Chile
- Zsarnóczay Á (2013) Experimental and numerical investigation of buckling restrained braced frames for eurocode conform design procedure development. In: Department of structural engineering. Budapest University of Technology and Economics, Budapest
- McKenna F, Scott MH, Fenves GL (2010) Nonlinear finite-element analysis software architecture using object composition. J Comput Civ Eng 24(1):95–107
- ASCE 7 (2016) Minimum design loads and associated criteria for buildings and other structures (ASCE/SEI 7-16). American Society of Civil Engineers, Reston
- Simpson BG (2018) Design development for steel strongback braced frames to mitigate concentrations of damage. In: Civil and Environmental Engineering. University of California, Berkeley, Berkeley
- Uriz P, Mahin SA (2008) Toward earthquake-resistant design of concentrically braced steelframe structures. In: PEER report 2008/08. Pacific Earthquake Engineering Research Center, University of California, Berkeley, Berkeley

- 8. Merritt S, Uang C-M, Benzoni G (2003) Subassemblage testing of corebrace buckling-restrained braces. In: Final report to CoreBrace, LLC. University of California, San Diego, La Iolla
- 9. Soti R, Ho TX, Sinha A (2021) Structural performance characterization of mass plywood panels. J Mater Civ Eng 33(10):04021275